Aggregation and Photophysics of Rose Bengal in Alumina-Coated Colloidal Suspensions

by **Marta E. Daraio**[a])[b]) and **Enrique San Román***[a])

[a]) INQUIMAE/Departamento de Química Inorgánica, Analítica y Química Física, Facultad de Ciencias Exactas y Naturales, Universidad de Buenos Aires, Pabellón 2, Ciudad Universitaria, 1428 Buenos Aires, Argentina (phone: ++54-11-4576-3358; fax: ++54-11-4576-3341; e-mail: esr@qi.fcen.uba.ar)

[b]) Laboratorio de Química de Sistemas Heterogéneos, Departamento de Química, Facultad de Ingeniería, Universidad de Buenos Aires, Av. Paseo Colón 850, 1063 Buenos Aires, Argentina

Dedicated to Professor *André M. Braun* on the occasion of his 60th birthday

The absorption and emission properties of Rose Bengal (RB) have been studied in colloidal suspensions of positively charged alumina-coated silica nanoparticles (Sil). Experimental spectra can be rationalized by the existence of an equilibrium between aqueous monomers and only one adsorbed species. However, a simple partition or a *Langmuir*-type adsorption-aggregation equilibrium do not explain the observed results. No evidence regarding the existence of adsorbed monomers is found even at low surface coverage. Aggregation stops at the dimer level, though, at high enough dye concentrations, the surface coverage is almost complete. Comparative experiments performed on negatively charged silica nanoparticles show that monomers are the only species present in this case. Fluorescence experiments on Sil indicate that dimers are fluorescent. Laser excitation of adsorbed dye leads to the formation of RB radical cations, while the dye triplet state is not observed.

Introduction. – The study of systems composed of organic dyes supported on particulate materials is of interest both from the applied and the theoretical points of view. Photophysical and photochemical processes carried out in heterogeneous media have been the subject of different studies because of their potentiality in areas such as conversion and storage of light energy and photocatalysis [1–3]. A common problem found in this kind of system is the formation of dye aggregates, as aggregation usually impairs the photochemical response. It is known that planar organic dyes are prone to aggregate strongly when constrained to restricted environments, such as the interior of a micelle or the surface of a solid, where the local concentration increases.

Aggregation is normally evidenced by electronic spectroscopy, but, while straightforward methods can be used to characterize homogeneous or microheterogeneous systems, studies become complicated in heterogeneous systems for a number of reasons. The existence of different phases or microphases obscures the interpretation of spectroscopical data, as aggregation can take place in more than one phase. Furthermore, heterogeneous systems are normally complicated by the occurrence of light dispersion. The nature of the interaction between dye and solvent and between dye and solid not only determines the partition equilibrium of the dye but also the degree of aggregation. As a result, a single dye can behave in entirely different ways on different solids suspended in the same solvent, and similar dyes can show different behaviors in identical environments.

As an example of the latter point, we recently studied systems composed of aluminum tetracarboxyphthalocyanine [4] and pheophorbide-a [5] adsorbed on microcrystalline cellulose. Both dyes are hydrophobic planar macrocycles that aggregate strongly in water.

Inorganic oxides, particularly nonreactive surfaces like silica or alumina, provide a bidimensional environment that modifies the properties of different adsorbed substrates [6][7]. Conversely, adsorbed substrates, particularly dyes, can yield valuable information regarding the surface properties of the support material [8]. The photophysical and photochemical properties of aggregates bound to SiO_2 colloids have been investigated for *Rhodamine 6G* [9] and cresyl violet [10].

For several years, we have investigated the properties of dyes, particularly phthalocyanines, adsorbed or chemically linked to solid substrates [4][5][11–14]. As a rule, phthalocyanines show, on adsorption, a strong tendency to form photochemically inactive dimers and higher aggregates. This process is favored in aqueous suspension due to the highly hydrophobic core of the dye.

Therefore, we were interested in the comparison between the behavior of these compounds with dyes showing a hydrophilic nature, and we selected Rose Rengal (RB) as a candidate. The selected support, alumina-coated colloidal silica particles with diameters in the nanometer range, is positively charged in weakly acidic medium (pH 4) and electrostatically attracts anionic molecules such as RB. Moreover, the small particle size allows formation of stable colloidal suspensions with negligible light dispersion. The system can thus be studied by conventional steady-state and time-resolved spectroscopic and photophysical methods.

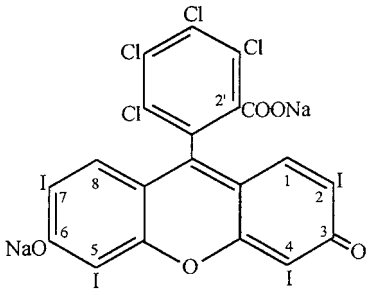

RB is an anionic water-soluble photosensitizer with a strong absorption band at *ca.* 550 nm [15][16] that aggregates in aqueous solution only at concentrations higher than 5×10^{-5} M [17]. The derivative Rose Bengal C(2′)ethyl ester C(6) sodium salt dimerizes at concentrations higher than 3×10^{-5} M in H_2O with 2% EtOH. Addition of KNO_3 [18] and other alkali metal salts [19] induces dimerization at much lower concentrations. The shape of the dimer absorption spectrum depends strongly on the nature of the cation.

The spectroscopic effects of aggregation have been studied in specially designed covalently linked RB derivatives containing two dye moieties separated by CH_2 chains of different lengths [20]. The location and intensity of absorption bands are a function of the solvent composition ($EtOH/H_2O$ at variable ratios). Furthermore, these

compounds exist in an open conformation in EtOH, but form dimers in aqueous solution.

The absorption and emission properties of RB have been also characterized on SiO_2, Al_2O_3 (nonreactive) and TiO_2 (reactive) particles. The diffuse reflectance spectra of RB on these particles showed a shoulder at *ca.* 500 nm, which was attributed to the ground-state dimer [6].

This work, therefore, presents data on the aggregation and photophysical behavior of RB in aqueous alumina-coated silica colloidal suspensions. The mechanism of association of RB to these particles is discussed, and excited states and transient species are examined by fluorescence and laser flash photolysis.

Experimental. – *Chemicals.* RB was obtained from *Aldrich* and used as supplied. An aq. colloidal suspension, *Nalco 1056*, of positively charged alumina-coated silica particles with average particle size of 20 nm, containing 26% (*w*/*w*) SiO_2, 4% (*w*/*w*) Al_2O_3, and 70% H_2O (pH 4.2, density 1.23 $g \cdot cm^{-3}$), was obtained from *Nalco Chemical Co.* (Naperville, IL). This suspension was diluted with 1×10^{-4} M HCl to obtain the desired particle concentrations while maintaining the excess positive surface charge. The particulate fraction will be hereafter referred to as Sil, the calculated density of which is expressed in $g \cdot dm^{-3}$. For comparative experiments in the presence of negatively charged silica particles, *Ludox AM30* (*Dupont*) with average particle size 12 nm containing 30% (*w*/*w*) SiO_2 (density 1.21 $g \cdot cm^{-3}$, surface modified with aluminum, creating a fixed negative charge independent of pH) was used. Experiments were performed on freshly prepared samples, though suspensions were found to be stable. A *Milli-Q* system was used to purify H_2O; all other chemicals were analytical reagents.

Methods. Absorption spectra were measured with a *Shimadzu 210-A* spectrophotometer. Fluorescence spectra were obtained on a *PTI Quantamaster* luminescence spectrometer. Laser flash photolysis experiments were carried out with a Nd : YAG (*Spectron Lasers*, 8 ns FWHM) with an excitation wavelength of 532 nm and detection of absorption by a 100 W tungsten-halogen lamp, a monochromator, and a *Hamamatsu R928* photomultiplier. The signals were digitized and averaged with a *HP54502* digital oscilloscope. All experiments were performed at r.t. ($23 \pm 2°$). The transparency of colloidal suspensions facilitated direct detection of the transient species.

Results and Discussion. – *Interaction of RB with Colloidal SiO_2/Al_2O_3 Particles.* Absorption spectra were obtained for RB aqueous solutions containing varying amounts of suspended Sil. As an example, results obtained for $[RB] = 2.0$ μM and Sil concentrations of $0 - 4.24 \times 10^{-2}$ $g \cdot dm^{-3}$ are shown in *Fig. 1*. In different series of experiments, similar results were obtained. Alternatively, the concentration of particles was held constant at $5 \times 10^{-3} - 2.4 \times 10^{-2}$ $g \cdot dm^{-3}$ while the concentration of RB was varied from 7.1×10^{-7} to 4.76×10^{-6} M. As before, different series of experiments yielded similar results when both sample and reference cuvettes contained the same concentration of colloidal particles.

For a given set of experimental conditions, suspensions prepared by adding a RB solution to a Sil suspension or *vice versa* and at different mixing rates showed the same absorption spectrum. Results point to the existence of an adsorption equilibrium in which dye molecules are free to exchange between colloidal particles.

As expected, the spectrum obtained in the absence of Sil (*Fig. 1*, *Spectrum a*) is consistent with the reported spectrum of aqueous monomeric RB [17]. Under our experimental conditions, its shape is independent of the concentration of RB, and the *Lambert-Beer* law holds. As the concentration of Sil increases, a limiting spectrum is approached (*Fig. 1*, *Spectrum b*). These observations and the presence of clean isosbestic points lead us to assume that the solution of monomeric RB is equilibrated

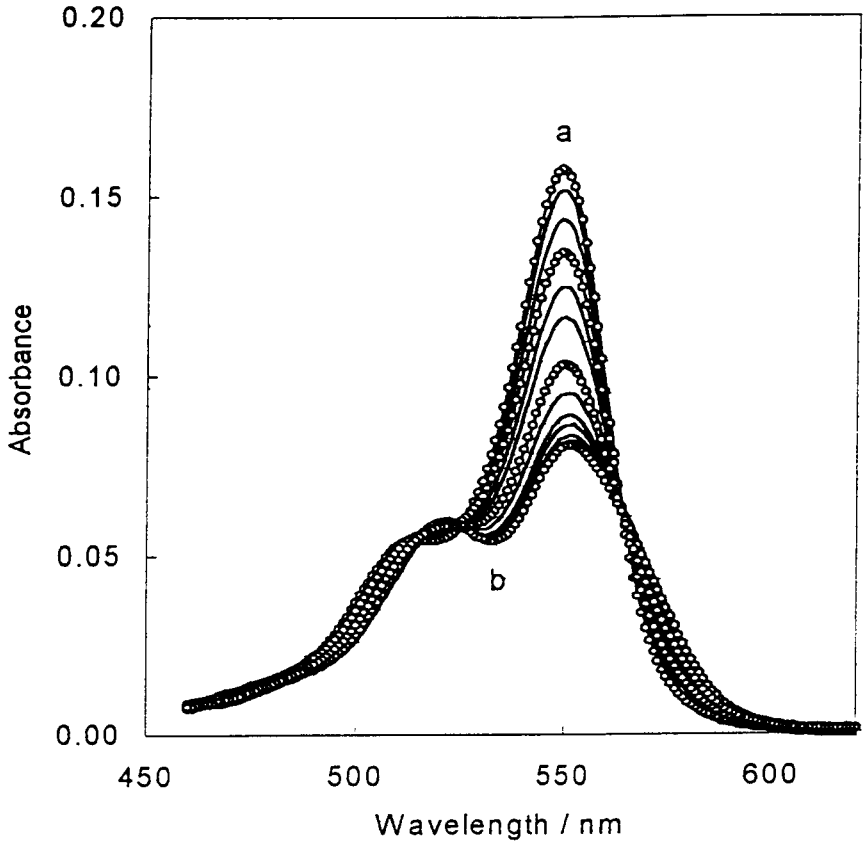

Fig. 1. *Absorption spectra of suspensions of RB on Sil.* [RB] = 2.0 μM, Sil at 0 (*Spectrum* 'a'), 0.12, 0.25, 0.37, 0.49, 0.61, 0.86, 1.10, 1.34, 1.59, 1.83, 2.07, 2.56, 3.16, an 4.24×10^{-2} (*Spectrum* '*b*') $g \cdot dm^{-3}$ in both sample and reference. Optical path length: 1 cm. Solid lines: experimental spectra, open circles: calculated spectra (see text).

with only one kind of adsorbed species and that, at high enough concentration of Sil, all RB molecules are adsorbed. These assumptions will be validated later.

The band structure of the limiting spectrum is consistent with this species being a lower aggregate of RB [13]. However, the possibility that the adsorbed species may be a monomer, the spectrum of which is drastically modified by the surface, is not excluded for the moment. Thus, the simplest but quite general model that explains this behavior is:

$$n\ M_a + Sil = M_{n,p} \tag{1}$$

where M_a represents the monomer in the aqueous phase and $M_{n,p}$ the n-aggregate (or the monomer for $n = 1$) adsorbed on the particle. In the following discussion, $[M_a]$ and $[M_{n,p}]$ are expressed in $mol \cdot dm^{-3}$, and $[M_{n,p}]$ represents the bulk concentration of the adsorbed species.

Concentration of Dissolved and Adsorbed RB. The calculation of the concentrations of the aqueous monomer and the adsorbed species for a given sample is possible if both spectra are known. We can obtain the monomer spectrum in the aqueous phase from *Fig. 1* in the absence of Sil. On the other side, by increasing the concentration of Sil, as stated before, a constant spectrum is obtained for the adsorbed species at infinite densities of Sil. Although this approach is entirely valid, a somewhat more involved treatment will be applied. Through this approach, all experimental data is globally analyzed to obtain the required spectra, thus minimizing errors, while the method allows a number of consistency tests to be made.

Absorbance may be considered a bilinear form of absorption coefficients and concentrations: by a matrix formalism [21]:

$$[A_{\lambda s}] = ([\varepsilon_\lambda] \times [c_s]) + [d_{\lambda s}] \tag{2}$$

Each column of the absorbance matrix $[A_{\lambda s}]$ contains the experimental absorption spectrum of a given sample, $[\varepsilon_\lambda]$ is a matrix whose columns contain the absorptivities of the different species, and $[c_s]$ is a matrix, whose columns contain the concentrations of the same species for a given sample. The optical pathlength (1 cm) is implicit. The aim of the calculation is to minimize the terms of the error matrix $[d_{\lambda s}]$ by means of a regression procedure as described in [21].

Typically, *Eqn. 2* can be used to calculate matrix $[c_s]$ from a known matrix $[\varepsilon_\lambda]$ or *vice versa*. The calculation has the advantage over standard procedures that all spectral information is used rather than only absorbance maxima. Moreover, this equation can be also of value in cases where knowledge of $[\varepsilon_\lambda]$ and $[c_s]$ is only partial or even when no data other than the experimental absorbances are given. In the last case, starting from an arbitrary matrix $[\varepsilon_\lambda]$, a matrix $[c_s]$ may be calculated, from which a new matrix $[\varepsilon_\lambda]$ is obtained, and so on. The process may be iteratively repeated until convergence is reached. At this end, the product of the matrices $[\varepsilon_\lambda] \times [c_s]$, while individually arbitrary, yields an optimized absorbance matrix that differs from the experimental one in that random error is suppressed. Typically, the starting matrix $[\varepsilon_\lambda]$ is composed of a number of columns – which equals the proposed number of species – of the experimental absorbance matrix divided by the analytical concentration of RB.

When the proposed number of species is too low, the adjustment between optimized and experimental absorbance matrices is poor. When a larger number of species is assumed, the adjustment is good but calculation of $[\varepsilon_\lambda]$ and $[c_s]$ yields erratic results. This is to be expected because the regression procedure calculates the elements of those matrices as a quotient of determinants that nearly vanish when the number of species is overestimated. *Fig. 1* shows the agreement between experimental and optimized absorbances for selected samples, assuming the existence of two species. Similar results are obtained for all samples.

The concordance between experimental and optimized absorbance matrices is excellent, so that experimental absorbance data can be considered a combination of two independent spectra. This does not exclude the possible existence of more than one species sharing the same spectrum but, as it will be demonstrated later, this is not likely to be the case.

Once absorbances are optimized, a new matrix $[\varepsilon_\lambda]$ is obtained by replacing its columns with selected columns of the optimized absorbance matrix divided by the analytical concentration of RB. These columns correspond to RB in H_2O with no Sil present and to a sample with a large amount of Sil, for which it may be assumed that only the adsorbed species is present. The corresponding spectra are shown in *Fig. 2*.

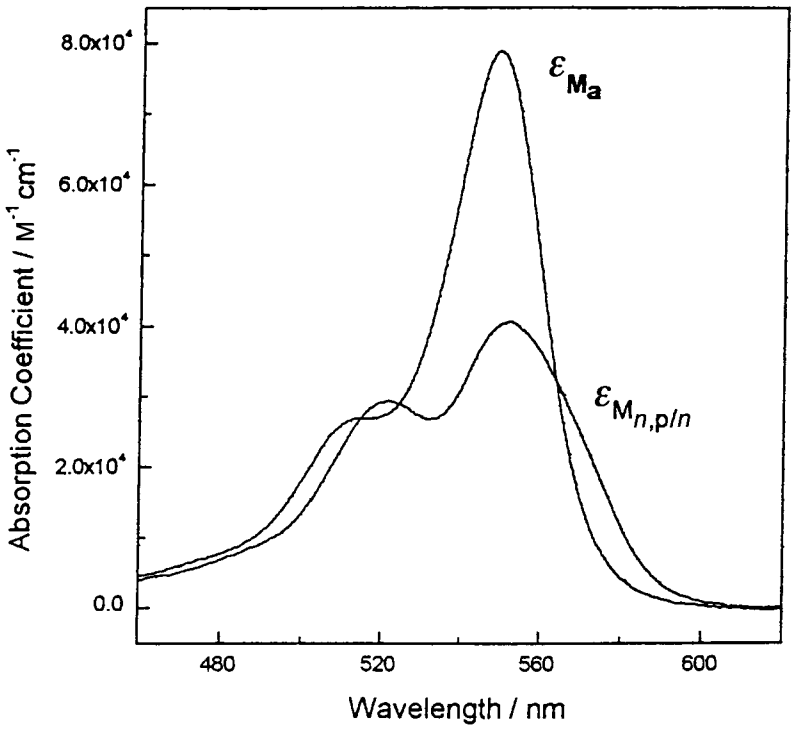

Fig. 2. *Absorption spectra of RB aqueous monomer* (ε_{M_a}) *and adsorbed species* (per monomer unit, $\varepsilon_{M_{n,p}}/n$)

Starting from the newly obtained $[\varepsilon_\lambda]$ matrix, a new concentration matrix is calculated, the rows of which represent the concentration of the two independent species as a function of the sample. Concentrations obtained in this way for samples at constant $[RB] = 2 \times 10^{-6}$ M are represented in *Fig. 3* as a function of the amount of Sil.

It is clear from this figure that the two species are stoichiometrically related, as the sum of concentrations equals the analytical concentration of RB, and that the adsorbed species reaches a plateau as the amount of Sil increases. It should be noted, however, that only $\varepsilon_{M_{n,p}}/n$ and $n \cdot [M_{n,p}]$ are obtained, as the aggregation number cannot be determined in this way.

That a plateau is reached in *Fig. 3* for the concentration of the adsorbed species indicates that only two species exist. In fact, the above treatment does not exclude that both monomers and aggregates coexist on the surface, provided that the spectrum of the adsorbed monomer coincides in shape and in amplitude with that of the monomer in solution. However, this would imply that the equilibrium between monomers and

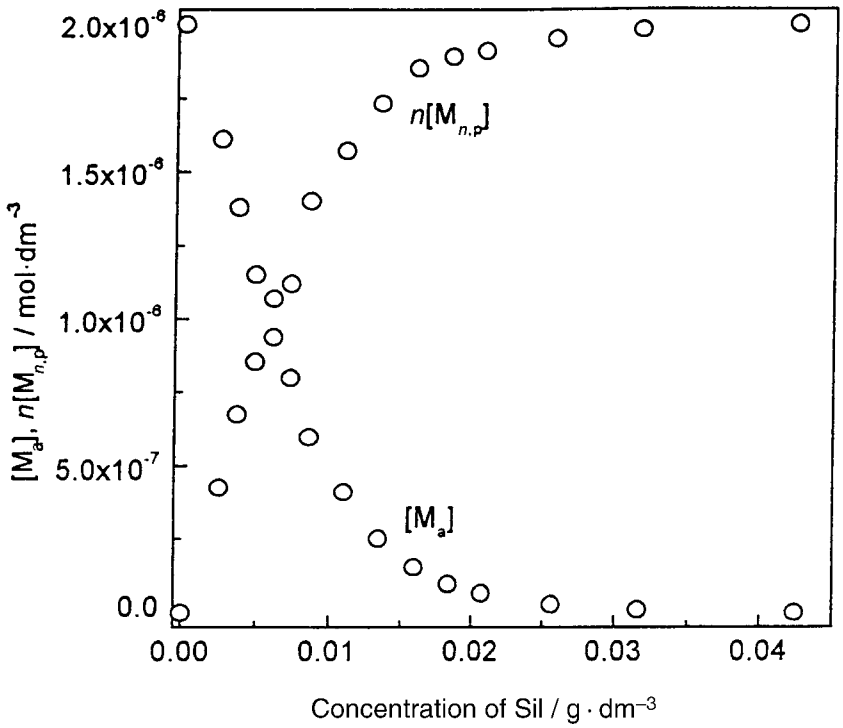

Fig. 3. *[M_a] and* n*[$M_{n,p}$] at constant [RB]* (2 μM) *as a function of Sil concentration*

aggregates would be shifted in direction of the monomeric state as the amount of Sil increases, so that the limiting spectrum at high enough amounts of Sil would be that of the monomer, which is clearly not the case.

Characterization of the Adsorbed Species. Two limiting situations were analyzed to investigate the association equilibrium: *a*) partitioning of RB between H_2O and Sil and *b*) binding of RB to a definitive number of surface sites. A complex dependence of $[M_{n,p}]/[M_a]^n$ on Sil was observed for different n values. Therefore, a simple partition equilibrium can be ruled out and a binding mechanism:

$$n\ M_a + Sil_{free} = M_{n,p} \tag{3}$$

where Sil_{free} characterizes free sites on the Sil surface, must be considered.

Where N is the maximum number of moles of the adsorbed species that can be associated with 1 g of Sil particles (in $mol \cdot g^{-1}$) and N[Sil] the maximum attainable bulk molarity at a given Sil concentration, the fraction of occupied binding sites is $\theta = [M_{n,p}]/N[Sil]$. *Fig. 4* represents $n[M_{n,p}]/[Sil] = nN\theta$ as a function of $[M_a]$.

It may be observed from *Fig. 4* that a limiting value is obtained for the fraction of occupied sites. This shows that the binding hypothesis is justified and that a partitioning mechanism must be excluded. Assuming $\theta = 1$ at large enough $[M_a]$, a value $nN = 1.8 \times 10^{-4}\ mol \cdot g^{-1}$ follows.

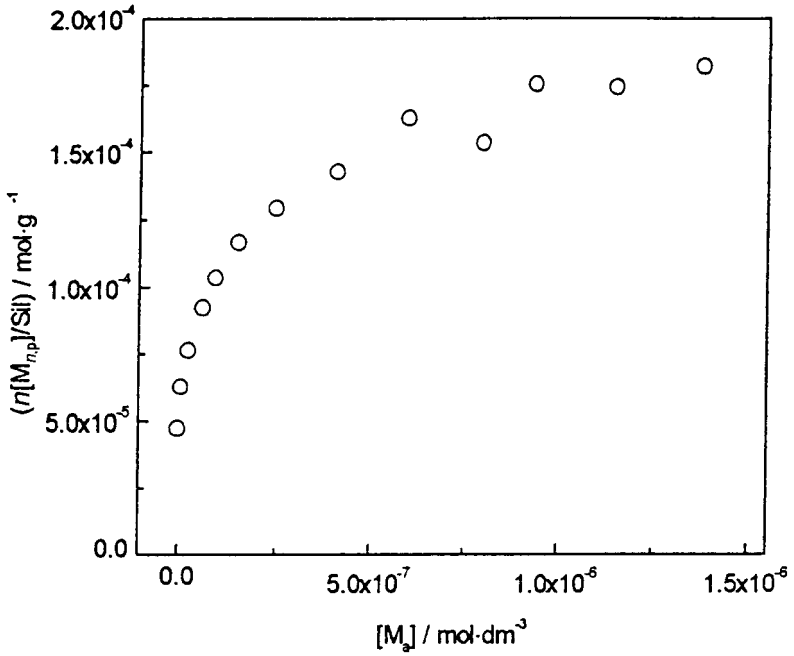

Fig. 4. n$[M_{n,p}]/Sil$ *at constant [RB]* (2 μM) *as a function of* $[M_a]$

If a *Langmuir*-type adsorption-aggregation equilibrium is assumed, the following expression for the association constant K (in M^{1-n} $(g \cdot dm^{-3})^{-1}$) is obtained:

$$K = \frac{[M_{n,p}]}{[M_a]^n \ ([Sil] - [M_{n,p}]/N)} \tag{4}$$

On testing *Eqn. 4* at different n values, a dependence of K on θ is obtained in all cases. In fact, from *Fig. 4*, it may be observed that $nN\theta$ increases sharply at low $[M_a]$ and slowly at higher concentrations. Thus, a simple *Langmuir*-type equilibrium is not fulfilled either because sites of different kinds are involved or because interaction between adsorbed species cannot be disregarded. Therefore, the aggregation number cannot be obtained in this way.

The spectrum of the adsorbed species shows two bands located at 521 and 552 nm with a ratio of these absorbance maxima of 0.72. The lower-energy band is red-shifted compared to the main band of the monomer, which is located at 549 nm. The observed differences show that the adsorbed species cannot be a monomer. In fact, it is well-known that the spectrum of RB in solution changes dramatically on aggregation [17], and, in most cases, aggregation is evidenced through an increase of absorption at wavelengths shorter than that of the monomer band [22][23].

In homogeneous solution, one of the few examples found in the literature concerns the Rose Bengal C(2)-ethyl ester C(6) sodium salt in 2% EtOH in the presence of KNO_3 [18][19]. The spectrum, attributed in this case of the dimeric species, shows

absorption maxima at 526 and 572 nm with an intensity ratio of 1.1. The monomeric compound, obtained in the absence of salt, shows only one maximum at 554 nm with a satellite band at 516 nm. These values can be compared with those obtained in our case for the adsorbed and the dissolved (monomeric) species. While the monomer spectrum of the ester differs only slightly from the spectrum of monomeric RB, the main band of the dimer is red-shifted to a large extent.

Several dyes show minor spectral changes on absorption, and, therefore, their spectra are assigned to the monomeric species. As an example, the spectrum of 2,2′-azinobis(3-ethyl-benzothiazoline-6-sulfonate) changes only its intensity on adsorption on Sil particles [24]. In the case of anthracene-1,5-disulfonate and anthracene-1-sulfonate on the same support, almost no changes are observed [25].

To obtain further evidence, we studied the behavior of RB in the presence of negatively charged particles. *Fig. 5* shows results obtained for a fixed concentration of RB (2.0 μM) and varying amounts of *Ludox AM30* (0 to 4.2×10^{-2} g · dm^{-3}). In this case, the behavior is similar to that obtained for the benzothiazoline dye cited above. Clearly, no aggregation is evidenced when RB is adsorbed on negatively charged *Ludox*.

As has been found for xanthene dyes [18], dimeric species show two absorption maxima located at both sides of the monomer absorption maximum. The splitting is

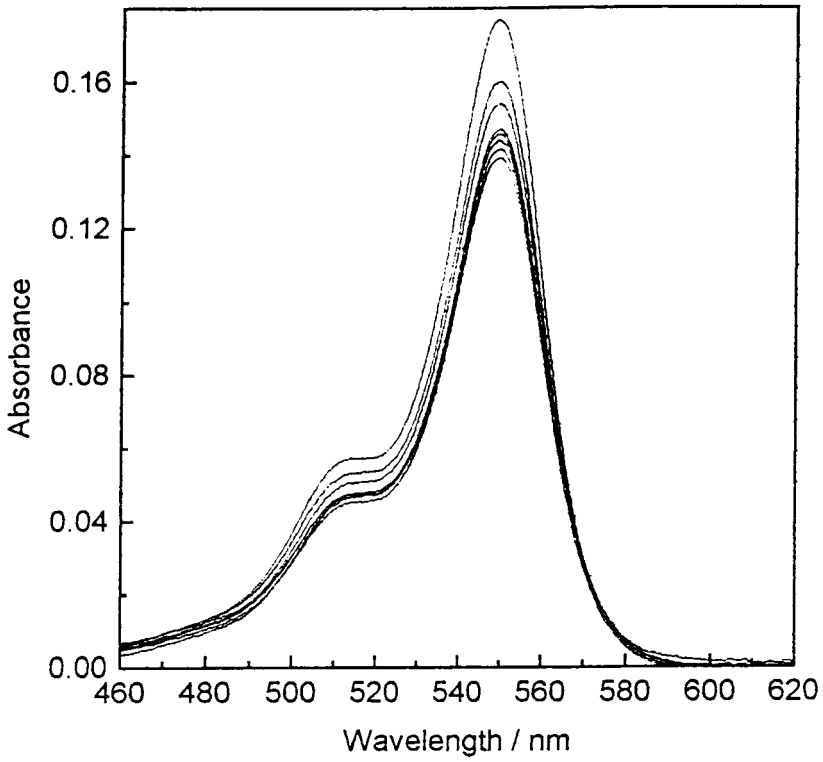

Fig. 5. *Absorption spectra of RB in the presence of* Ludox (negatively charged silica particles). [RB] = 2 μM. *Ludox* at 0, 0.24, 0.48, 0.84, 1.2, 1.8, 3.0, and 4.2×10^{-2} g · dm^{-3}.

caused by excitonic interaction between the monomeric units [26]. According to exciton theory, a sandwich structure (H-aggregate) shows only one blue-shifted band while a single red-shifted band is indicative of a coplanar structure (J-aggregate). Two bands only are allowed for angular structures, and the short-to-long-wavelength band ratio correlates with the angle between the transition dipoles of the monomeric units. For xanthene dyes, the short-wavelength band is normally of higher intensity [22][23], pointing to monomers that are nearly face to face. The reverse is found for derivatives of RB that have a cation such as tributylammonium at C(6), which may be explained by assuming an angle between 90 and 180° [20]. *Fig. 2* shows that the latter should be the case for RB adsorbed on Sil.

We conclude, therefore, that the adsorbed species is a dimer in our case. According to the reported results, dimers are the only adsorbed species even at submonolayer coverage. This behavior has also been observed for anthracene-2-sulfonate on Sil [25].

The number of sites on the Sil particles bears some relationship to the number of surface charges. The reported specific surface area of Sil particles is $102\ m^2 \cdot g^{-1}$ [24]. Considering that the adsorbed species is a dimer, a value of $N = 9 \times 10^{-5}\ mol \cdot g^{-1}$ is found from the results shown in *Fig. 4*. Therefore, a density of sites of $9 \times 10^{-5}\ mol \cdot g^{-1}/102\ m^2 \cdot g^{-1} = 8.8 \times 10^{-11}\ mol \cdot cm^{-2}$ can be calculated. This value represents 37% of the surface concentration of sodium dodecylsulfate ($2.4 \times 10^{-10}\ mol \cdot cm^{-2}$) that is required to reverse the ζ potential of α-alumina at pH 4.2 [27], suggesting that more than two positive binding sites are needed to accommodate a dimer molecule with two or more negative charges. Obviously, charge compensation stabilizes the dimeric state. This is not possible in the case of negatively charged *Ludox*.

From the density of sites, the minimum surface available for a dimer molecule can be calculated as $1.88\ nm^2$. For a square lattice, the minimum distance between the centers of two consecutive dimers would then be 1.37 nm, high enough for them to be considered isolated from each other. Assuming a C–C bond length of about 0.14 nm, a monomer cross section of about $0.5\ nm^2$ can be calculated. Thus, a coplanar dimer would occupy nearly half of a cell. For angular dimers, the occupancy factor would be lower. The available space increases with the ratio of Sil/[RB]. For example, at the highest ratio used in this work, the available area is $7.1\ nm^2$ per dimer molecule.

The effect of charges on dimerization has been observed in the previously discussed example of the RB ethyl ester [18][19]. In the case of the ester, aggregation is induced by interaction between the anion of the dye and added electrolyte. In our case, that the spectrum of monomeric aqueous RB does not change in the presence of NaCl or KNO_3 and that *Ludox* does not induce aggregation demonstrates that the specific role of the surface charge is neutralization. Once a single monomer is adsorbed on Sil, compensation of charges allows a second monomer to be adsorbed to generate a dimeric species.

Laser Flash Photolysis. A deoxygenated suspension with Sil present at $43\ g \cdot dm^{-3}$ and [RB] = 88 μM (2.0 μmol RB/g Sil), in which the adsorbed species exceeds 99% of total RB, was excited at 532 nm. The amounts of Sil and RB are high enough to obtain a measurable transient signal. This sample yielded no detectable signal in the region of 600–700 nm, where the triplet state of RB adsorbed on dry SiO_2 or Al_2O_3 has a broad absorption maximum [6]. Only at high laser intensities (*ca.* 300 mJ/pulse) was a transient with maximum absorbance at 470 nm observed. This transient is present both

in deaereated and in O_2-saturated samples. These observations rule out the presence of the triplet state. The difference absorption spectrum, shown in *Fig. 6*, is similar to the spectrum reported for $RB^{+\bullet}$ in aqueous solution [28]. The semioxidized radical has a decay time of around 30–50 ms.

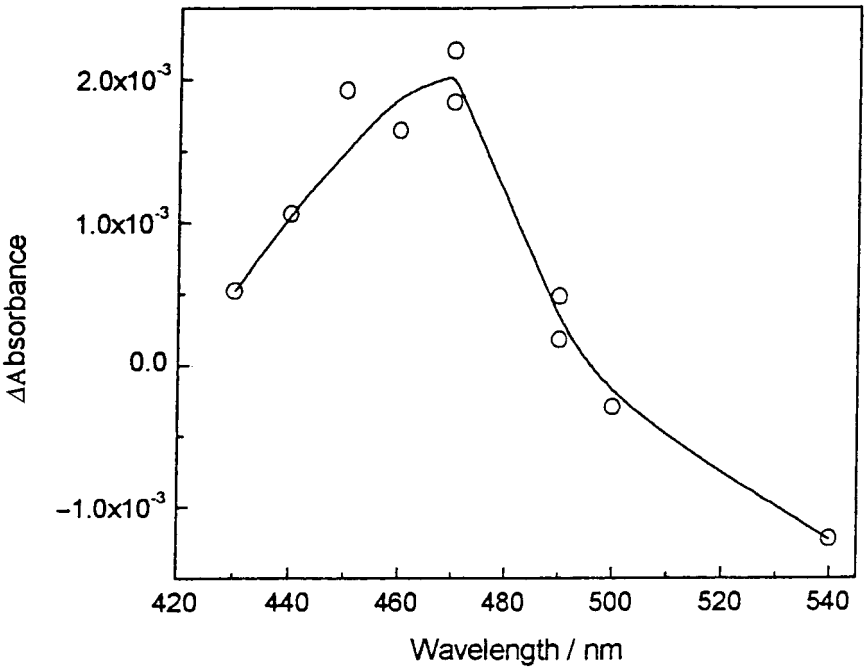

Fig. 6. *Transient absorption recorded following a 532 nm laser excitation* (energy about 300 mJ per pulse, Sil at 43 $g \cdot dm^{-3}$, and [RB] = 88 μM)

The formation of $RB^{+\bullet}$ was reported on Al_2O_3 surfaces in solid media [6]. It was thought to be the result of a photoionization process:

$$^3RB \text{ (or } ^1RB) + h\nu \rightarrow RB^{+\bullet} + e^- \quad (5)$$

Lewis acid sites on the Al_2O_3 surface are strong electron acceptors that facilitate photoionization. However, since, in our case, the triplet state is not observed and the laser pulse width must be much larger than the singlet lifetime render this explanation unlikely. Other possible explanations would be a low quantum efficiency in the monophotonic excitation of dimers or the excitation of a very small amount of adsorbed monomers. Both are consistent with a prevalence of aggregates on the Sil surface.

Fluorescence. Fig. 7 shows fluorescence spectra of RB in the presence of different amounts of Sil. The excitation was at 513 nm, which is an isosbestic point for the absorption of the monomeric and aggregated forms of the dye.

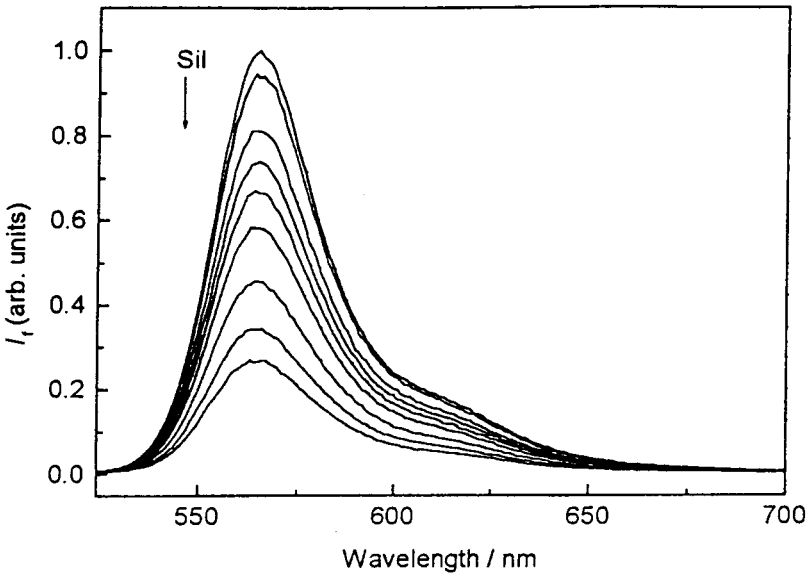

Fig. 7. *Fluorescence spectra of suspensions of RB on Sil.* [RB] = 2.0 μM, Sil at 0, 0.24, 0.50, 0.61, 0.74, 0.86, 1.10, 1.34, and 1.58×10^{-2} g · dm^{-3}, excitation at 513 nm.

The addition of particles leads to a noticeable decrease in emission intensity. The maximum remains at (565 ± 2) nm, a value that can be compared with fluorescence maxima observed for RB adsorbed on Al_2O_3 (570 nm) and on SiO_2 (562 nm) [6].

In a system containing two fluorescent species, monomers (M) and dimers (D), following equation applies [29]:

$$\frac{I_f/I_o}{(1-10^{-A})\gamma_M} = \phi_M + \phi_D \frac{\gamma_D}{\gamma_M} \tag{6}$$

where I_f and I_o are the emitted and the incident photon fluxes, respectively, expressed in the same units, ϕ_M and ϕ_D are the fluorescence quantum yields corresponding to the monomer and the dimer, respectively, and γ_M and γ_D are the fractions of incident light absorbed by the corresponding species, calculated as:

$$\gamma_M = \frac{\varepsilon_{M_a}\,[M_a]b}{A} \tag{7}$$

and:

$$\gamma_D = \frac{\varepsilon_{D_p}[D_p]b}{A} \tag{8}$$

In the above equations, b is the optical pathlength and A, ε_{M_a}, and ε_{D_p} are taken at the excitation wavelength.

Fig. 8 shows fluorescence data treated according to *Eqn. 6*. In spite of the nonlinearity, the observed dependence on γ_D/γ_M suggests that ϕ_D is not zero. In general, coplanar aggregates may be fluorescent while excited sandwich structures deactivate

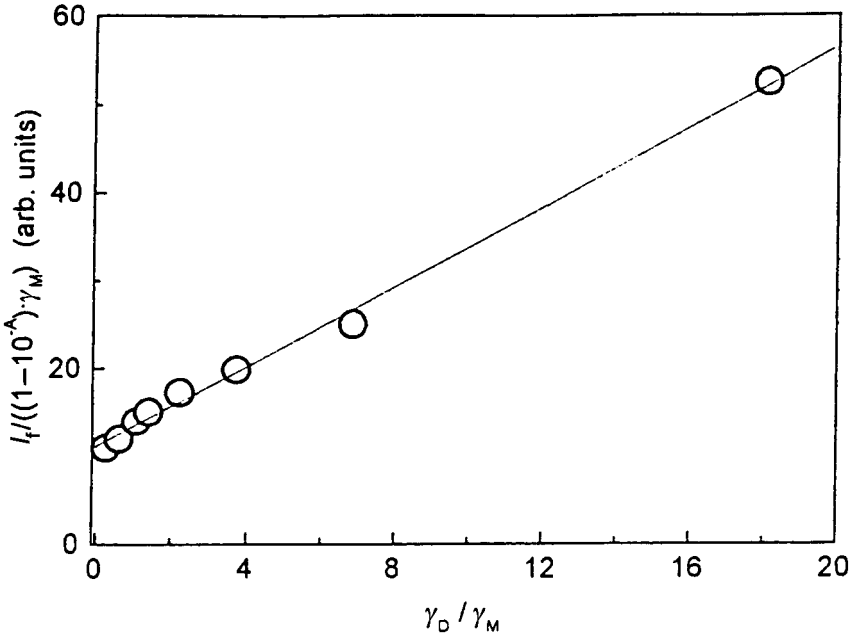

Fig. 8. *Fluorescence data treated according to* Eqn. 6

rapidly, leading to nondetectable fluorescence levels. This may be taken as further evidence of the angular geometry of the dimers. It should be noted that no new emission band arises from the dimeric state. Moreover, excitation spectra resemble the monomer absorption spectrum. Rather similar behavior was found for a bisphthalocyanine condensed through a common benzene ring [30], for which the excitation spectrum resembles more the absorption spectrum of the isolated monomer than that of the condensed dimer.

Conclusions. – Positively charged Sil nanoparticles cause negative RB molecules to dimerize on the surface irrespective of the ratio of the Sil density to [RB]. Compared to the monomer spectrum, the spectrum of the dimer is shifted to higher wavelengths. This and the observed band ratio suggest an angular structure for the dimer. The fraction of occupied sites reaches a limiting value at low amounts of Sil per [RB], thus excluding a partitioning equilibrium and pointing to a binding adsorption mechanism. The number of available sites is such that more than two positive charges are needed on the surface to compensate for the charge of the dimer. This helps to stabilize the dimeric structure. The available space for each dimer molecule amounts to nearly four times the area of a monomer, with a distance between centers of the adsorbed dimers of about 1.4 nm. This allows each dimer to be considered a separate entity. Comparative experiments performed with RB on negatively charged *Ludox AM30* nanoparticles show that the adsorbed species are dye monomers in this case. Therefore, surface charge is a relevant factor in deciding the state of the dye on the surface.

Flash-photolysis experiments performed for RB on Sil do not show the presence of the triplet state, a result that is consistent with surface dimerization. Instead, trace amounts of dye radical cations are observed, pointing to the occurrence of injection of charge into the particle matrix. However, evidence of dimer fluorescence is found, reinforcing the hypothesis that the dimers are almost coplanar.

E.S.R. is member of *the Carrera del Investigador Científico y Tecnológico de CONICET* (Argentina). This work was supported by the *European Union* (Project ERBIC18CT96076), *CONICET* (PIP 0661/98), *ANPCyT* (PICT 06-03613, BID 802/OC-AR), the University of Buenos Aires (UBACyT TX43), and *Fundación Antorchas.*

The authors wish to thank to Dr. *Daniel A. Fernández* for flash-photolysis measurements.

REFERENCES

[1] K. Kalyanasundaram, 'Photochemistry in Microheterogeneous Systems', Academic Press, New York, 1987.
[2] V. Ramamurthy, 'Photochemistry in Organized and Constrained Media', VCH, New York, 1991.
[3] 'Studies in Surface Science and Catalysis, Photochemistry on Solid Surfaces', Eds. M. Anpo, T. Matsura, Elsevier, Amsterdam, 1989, Vol. 47.
[4] M. G. Lagorio, L. E. Dicelio, M. I. Litter, E. San Román, *J. Chem. Soc., Faraday Trans.* **1998**, *94*, 419.
[5] A. Zeug, J. Zimmermann, B. Röder, M. G. Lagorio, E. San Román, *Phys. Chem. Chem. Phys.* **2001**, *3*, 1524.
[6] K. R. Gopidas, P. V. Kamat, *J. Phys. Chem.* **1989**, *93*, 6428.
[7] P. V. Kamat, *Chem. Rev.* **1993**, *93*, 267.
[8] J. K. Thomas, *J. Phys. Chem.* **1987**, *91*, 267.
[9] C. Nasr, D. Liu, S. Hotchandani, P. V. Kamat, *J. Phys. Chem.* **1996**, *100*, 11054.
[10] D. Liu, G. L. Hug, P. V. Kamat, *J. Phys. Chem.* **1995**, *99*, 16768.
[11] E. San Román, *J. Photochem. Photobiol. A, Chem.* **1996**, *102*, 109.
[12] J. Hodak, C. Quinteros, M. I. Litter, E. San Román, *J. Chem. Soc., Faraday Trans.* **1996**, *92*, 5081.
[13] J. L. Bourdelande, M. Karzazi, G. Marqués Tura, L. E. Dicelio, M. I. Litter, E. San Román, V. Vinent, *J. Photochem. Photobiol, A, Chem.* **1997**, *108*, 273.
[14] E. San Román, J. A. Navío, M. I. Litter, *J. Adv. Oxidation Technol.* **1998**, *3*, 261.
[15] D. C. Neckers, *J. Photochem. Photobiol. A, Chem.* **1989**, *47*, 1.
[16] H. Stiel, K. Teuchner, A. Paul, D. Leupold, I. Kochevar, *J. Photochem. Photobiol. B, Biol.* **1996**, *33*, 245.
[17] D. Xu, D. C. Neckers, *J. Photochem.* **1987**, *40*, 361.
[18] O. Valdés-Aguilera, D. C. Neckers, *J. Phys. Chem.* **1988**, *92*, 4286 and refs. therein.
[19] O. Valdés-Aguilera, D. C. Neckers, *J. Photochem. Photobiol. A., Chem.* **1989**, *47*, 213.
[20] D. K. Lutrull, O. Valdés-Aguilera, S. M. Linden, J. Paczkowski, D. C. Neckers, *Photochem. Photobiol.* **1988**, *47*, 551.
[21] E. San Román, M. C. González, *J. Phys. Chem.* **1989**, *93*, 3532.
[22] F. López Arbeloa, I. Llona González, P. Ruiz Ojeda, I. López Arbeloa, *J. Chem. Soc., Faraday Trans. II*, **1982**, *78*, 989.
[23] K. K. Rohatgi, A. K. Mukhopadhyay, *J. Phys. Chem.* **1972**, *76*, 3970.
[24] P. V. Kamat, W. E. Ford, *J. Phys. Chem.* **1989**, *93*, 1405.
[25] W. E. Ford, P. V. Kamat, *J. Phys. Chem.* **1989**, *93*, 6423.
[26] M. Kasha, H. R. Rawls, M. A. El-Bayoumi, *Pure Appl. Chem.* **1965**, *11*, 371.
[27] D. W. Fuerstenau, T. Wakamatsu, *Faraday Discuss. Chem. Soc.* **1975**, *59*, 157.
[28] C. Lambert, V. Sama, T. G. Truscott, *J. Chem. Soc., Faraday Trans.* **1990**, *86*, 3879.
[29] R. M. Negri, A. Zalts, E. San Román, P. F. Aramendıa, S. E. Braslavsky, *Photochem. Photobiol.* **1991**, *53*, 317.
[30] C. C. Leznoff, H. S. Lam, M. Marcuccio, W. A. Nevin, P. Janda, N. Kobayashi, A. B. P. Lever, *J. Chem. Soc., Chem. Commun.* **1987**, 699.

Received June 5, 2001